Lyapunov-Based MPC with Robust Moving Horizon Estimation and its Triggered Implementation

Jing Zhang and Jinfeng Liu
Dept. of Chemical and Materials Engineering, University of Alberta, Edmonton, AB T6G 2V4, Canada

DOI 10.1002/aic.14187
Published online July 29, 2013 in Wiley Online Library (wileyonlinelibrary.com)

In this work, we consider moving horizon state estimation (MHE)-based model predictive control (MPC) of nonlinear systems. Specifically, we consider the Lyapunov-based MPC (LMPC) developed in (Mhaskar et al., IEEE Trans Autom Control. 2005;50:1670–1680; Syst Control Lett. 2006;55:650–659) and the robust MHE (RMHE) developed in (Liu J, Chem Eng Sci. 2013;93:376–386). First, we focus on the case that the RMHE and the LMPC are evaluated every sampling time. An estimate of the stability region of the output control system is first established; and then sufficient conditions under which the closed-loop system is guaranteed to be stable are derived. Subsequently, we propose a triggered implementation strategy for the RMHE-based LMPC to reduce its computational load. The triggering condition is designed based on measurements of the output and its time derivatives. To ensure the closed-loop stability, the formulations of the RMHE and the LMPC are also modified accordingly to account for the potential open-loop operation. A chemical process is used to illustrate the proposed approaches. © 2013 American Institute of Chemical Engineers *AIChE J*, 59: 4273–4286, 2013

Keywords: process control, moving horizon estimation, model predictive control, nonlinear systems, chemical processes

Introduction

Model predictive control (MPC) is a control strategy that has been widely used in manufacturing industries because of its ability to incorporate constraints, to account for optimization considerations, and to handle nonlinearities. At each sampling time, MPC solves online a constrained optimization problem to obtain an optimal input trajectory that minimizes a given performance index.[1] MPC in general requires full knowledge of the state. However, in many cases, not all of the states are measurable. This makes the development of MPC based on output measurements very important. Unfortunately, a separation principle in general does not exist for nonlinear MPC. Existing output feedback nonlinear MPC results can be broadly classified into two categories. In the first category, a high-gain observer is in general used to estimate the system state which may allow semiglobal practical stability (e.g., Refs. 2 and 3). In the second category, observer errors are explicitly considered in the design of MPCs (e.g., Refs. 4–6) which requires that observer errors are bounded. For a review of output feedback MPC results, please refer to Ref. 7.

On the other hand, moving horizon estimation (MHE) has become a popular state estimation approach in recent years because of its ability to address nonlinearities and constraints (e.g., Refs. 8–11). In MHE, the state estimate is determined by also solving online an optimization problem.[8,12] The ability of MHE to handle constraints on process disturbances, measurement noise, and states was shown to lead to improved performance.[9] To account for historical data outside the estimation horizon, an arrival cost which summarizes the information of those data is included in the cost function of an MHE optimization problem. Different approaches have been developed to estimate the arrival cost.[8,13–16] In Ref. 9, sufficient conditions for asymptotic and bounded stability of MHE were established. However, in Ref. 9, the bounded stability was achieved based on a restrictive assumption on the approximation of the arrival cost. In a recent work,[17] a robust MHE (RMHE) scheme was developed based on an auxiliary nonlinear observer. The RMHE was proved to give bounded estimation error for nonlinear systems with bounded model uncertainties which is a desired property for an observer from a robust output feedback controller design point of view.

MHE-based output feedback MPC is an attractive approach as constraints, nonlinearities, and optimization considerations can be addressed in both state estimation and control. MHE-based MPC has been adopted in different applications including fast offset-free control system design,[11] control of solid oxide fuel cell,[18] and normalization of blood glucose.[19] A numerical method for simultaneous MHE and MPC via multiparametric programming was also developed.[20] However, in the above results, the stability of the closed-loop system was not established rigorously. In Ref. 21, MHE schemes with contractive constraints on the estimation error were proposed and based on the MHE schemes, robust output feedback MPC schemes were developed. However, the results in Ref. 21 were obtained without the consideration of constraints.

Motivated by the above observations, in this work, we develop MHE-based MPC schemes that give provable closed-loop stability for nonlinear systems with bounded uncertainties.

Corresponding concerning this article should be addressed to J. Liu at jinfeng@ualberta.ca.

In particular, we consider the RMHE developed in Ref. 17 as it gives bounded estimation error and the type of Lyapunov-based MPC (LMPC) developed in Refs. 22 and 23. The main idea of this type of LMPC is to formulate appropriate constraints in the MPC's optimization problem based on an auxiliary Lyapunov-based controller, in such a way that the MPC inherits the robustness and stability properties of the Lyapunov-based controller. One advantage of the LMPC is that it allows for an explicit characterization of the stability region and in general, has a reduced computational complexity.[22,23] Within the framework of the LMPC, designs for various classes of nonlinear systems and applications have been developed including constrained nonlinear control systems,[23] switched nonlinear control systems,[22] networked control systems with communicate data losses,[24] and time-varying delays,[25] distributed predictive control systems [26] as well as economic MPC.[6,27] However, all the previous results are based on the assumption that measurements of the entire system state are available except Ref. 3. In Ref. 3, a high-gain observer is used in the design of an output feedback economic MPC which requires the existence of a set of coordinates that can transform the nonlinear system to a linear system and does not take into account constraints or optimality in state estimation.

The objective of this work is twofold. In the first part, we focus on the case that the RMHE and the LMPC are evaluated every sampling time. In this case, an estimate of the stability region of the output feedback control system taking into account the estimation error explicitly is first established; and then sufficient conditions under which the closed-loop system with the output feedback control system is guaranteed to be stable are derived. RMHE and LMPC are both based on solving online optimization problems. For large-scale applications, the computational burden may be high. Thus, in the second part, we propose a triggered implementation strategy for the RMHE-based LMPC (RMHE-LMPC) to reduce the computational load of the system by reducing the evaluation times of the RMHE-LMPC. Triggered control has been used extensively in control systems that have shared resources, for example, shared communication and computation resources.[28–30] The triggering condition in this work is designed based on measurements of the output and its time derivatives. In order to ensure the closed-loop stability, the formulations of the RMHE and the LMPC are also modified accordingly to account for the potential open-loop operation time. Sufficient conditions for stability of the closed-loop system are also derived. The applicability and effectiveness of the proposed RMHE-LMPC designs are illustrated via the application to a chemical process.

Preliminaries

Notation

The operator $|\cdot|$ denotes Euclidean norm of a scalar or a vector, whereas $|\cdot|_Q^2$ indicates the square of the weighted Euclidean norm of a vector, defined as $|x|_Q^2 = x^T Q x$ where, Q is a positive definite square matrix. A function $f(x)$ is said to be locally Lipschitz with respect to its argument x if there exists a positive constant L_f^x such that $|f(x') - f(x'')| \leq L_f^x |x' - x''|$ for all x' and x'' in a given region of x and L_f^x is the associated Lipschitz constant. A continuous function $\alpha : [0, a) \to [0, \infty)$ is said to belong to class $\mathcal{K}$ if it is strictly increasing and satisfies $\alpha(0) = 0$. A function $\beta(r, s)$ is said to be a class $\mathcal{KL}$ function if for each fixed s, $\beta(r, s)$ belongs to class $\mathcal{K}$ with respect to r, and for each fixed r, it is deceasing with respect to s, and $\beta(r, s) \to 0$ as $s \to \infty$. The symbol $\mathrm{diag}(v)$ denotes a diagonal matrix whose diagonal elements are the elements of vector v. The symbol "\" denotes set substraction such that $\mathbb{A} \backslash \mathbb{B} := \{x \in \mathbb{A}, x \notin \mathbb{B}\}$. The superscript (s) denotes the s-th order time derivative of a function. The symbol $L_f h$ denotes the Lie derivative of function h with respect to f, defined as $L_f h(x) = \frac{\partial h}{\partial x} f(x)$, whereas $L_f^r h$ denotes r-th order Lie derivative, defined as $L_f^r h(x) = L_f L_f^{r-1} h(x)$.

System description

We consider a class of nonlinear systems that can be described by the following state-space model

$$\begin{aligned} \dot{x}(t) &= f(x(t), u(t), w(t)) \\ y(t) &= h(x(t)) + v(t) \end{aligned} \tag{1}$$

where $x \in \mathbb{R}^n$ is the vector of process state variables, $u \in \mathbb{R}^r$ denotes the control input vector, $w \in \mathbb{R}^p$ is the bounded state disturbance vector, $y \in \mathbb{R}^m$ is the measured output vector, and $v \in \mathbb{R}^m$ denotes the measurement noise vector. The input is restricted in a nonempty convex set $\mathbb{U} \subseteq \mathbb{R}^r$ which is defined as follows

$$\mathbb{U} := \{u \in \mathbb{R}^r : |u| \leq u_{\max}\} \tag{2}$$

where $u_{\max}$ is the magnitude of the input constraint. The disturbance and measurement noise vectors w and v are also bounded such that $w \in \mathbb{W}$ and $v \in \mathbb{V}$ where

$$\begin{aligned} \mathbb{W} &:= \{w \in \mathbb{R}^p : |w| \leq \theta_w\} \\ \mathbb{V} &:= \{v \in \mathbb{R}^m : |v| \leq \theta_v\} \end{aligned} \tag{3}$$

with θ_w and θ_v known positive real numbers. It it assumed that f and h are locally Lipschitz of their arguments and $f(0, 0, 0) = 0$ and $h(0) = 0$.

Modeling of measurements

We assume that the output of system (1), y, is sampled at time instants $\{t_{k \geq 0}\}$ such that $t_k = t_0 + k\Delta, k = 0, 1, \ldots$ with $t_0 = 0$ the initial time, Δ a fixed time interval and k positive integers. We also assume that measurements of the time derivatives of the output, $\dot{y}, \ldots, y^{(n-1)}$, are available at each sampling time. The two assumptions imply that a measurement of the following vector is available at each sampling time

$$Y(t) = \begin{bmatrix} y(t) \\ \dot{y}(t) \\ \vdots \\ y^{(n-1)}(t) \end{bmatrix} = \begin{bmatrix} h(x(t)) + v(t) \\ L_f h(x(t)) + \dot{v}(t) \\ \vdots \\ L_f^{n-1} h(x(t)) + v^{(n-1)}(t) \end{bmatrix} = \Phi(x(t)) + \phi(t) \tag{4}$$

where $\Phi(x) = \left[h(x)^T L_f h(x)^T \ldots L_f^{n-1} h(x)^T\right]^T$ and $\phi(t) = \left[v(t)^T \dot{v}(t)^T \ldots v^{(n-1)}(t)^T\right]^T$. The vector $\phi(t)$ denotes the uncertainties in the output and its derivative measurements. We further assume that the vector ϕ is bounded such that $\phi \in \mathbb{V}_2$ where

$$\mathbb{V}_2 := \left\{\phi \in \mathbb{R}^{nm} : |\phi| \leq \theta_\phi\right\} \tag{5}$$

with θ_ϕ a known positive number.

Note that the availability of the output time derivatives is only required in the design of the triggering condition of the

proposed RMHE-LMPC with triggered implementation. For the RMHE-LMPC evaluated every sampling time, it only requires the availability of the output measurements [i.e., $y(t)$].

Remark 1 *The assumption on the availability of output time derivatives is not a restrictive one from a practical point of view. The time derivatives can be approximated using numerical methods (e.g., finite difference methods) based on the current and previous output measurements and the approximation errors can be considered as additional measurement uncertainties. Note also that the boundedness of $\phi(t)$ requires that the change rate of measurement noise is sufficiently slow. However, this does not restrict the applicability of the proposed approach. A low-pass filter may be used to attenuate the high-frequency noise in the measurements before evaluating the derivatives like used in proportional-integral-derivative control.*[31] *Also, appropriate numerical methods including finite difference methods over one or several sampling periods and total variation regularization*[32] *can be used to significantly reduce the influence of the fast changing noise in the calculation of output derivatives. This point will be demonstrated in the application to a chemical process subject to bounded random measurement noise.*

Remark 2 *It is important to note that the assumption of availability of output time derivatives up to order $n-1$ can be relaxed for systems with multiple outputs. The minimum requirement is that the matrix composed of the derivative of the outputs and their time derivatives with respect to the system state (i.e., the observability matrix of the system which will be defined in (10) formally) is full rank. This point will also be demonstrated in the simulation studies.*

Stabilizability and observability assumptions

It is assumed that there exists a locally Lipschitz explicit nonlinear control law $u=k(x)$ that renders the origin of the nominal closed-loop system asymptotically stable while satisfying the input constraint for all x in a compact set $\mathbb{S}$ that contains the origin. Using the converse Lyapunov theorem,[33] this assumption implies that there exist a continuous differentiable control Lyapunov function $V(x)$ and $\mathcal{K}$ functions $\alpha_i, i=1,2,3$, satisfy the following conditions

$$\begin{aligned} &\alpha_1(|x|) \le V(x) \le \alpha_2(|x|),\\ &\frac{\partial V(x)}{\partial x} f(x,k(x),0) \le -\alpha_3(|x|),\\ &k(x) \in \mathbb{U} \end{aligned} \tag{6}$$

for all $x \in \mathbb{S}$. In the remainder, we will refer to a level set of V in $\mathbb{S}, \Omega_\rho$, as the stability region of the closed-loop system under the control law $k(x)$. The stability region Ω_ρ is defined as

$$\Omega_\rho := \{x \in \mathbb{S} : V(x) \le \rho\}. \tag{7}$$

Note that the above stability property of the nominal closed-loop system under the control law $k(x)$ is based on continuous state feedback and continuous implementation of the control action.

It is also assumed that the system is locally observable in Ω_ρ and that there exists a deterministic nonlinear observer for the nominal system of Eq. (1) which takes the following form

$$\dot{z}(t) = F(z(t), u(t), h(x)) \tag{8}$$

such that z asymptotically tracks x for all the states $z \in \Omega_\rho$ and $x \in \Omega_\rho$. In observer (8), z is the state vector of the observer, and $h(x)$ denotes the noise-free measurement of the output of the nominal system. This assumption implies that there exists a $\mathcal{KL}$ function β such that

$$|z(t)-x(t)| \le \beta(|z(0)-x(0)|, t) \tag{9}$$

for the nominal system with noise-free measurements for $z, x \in \Omega_\rho$. The vector function F is assumed to be locally Lipschitz with respect to its arguments. The above observability assumption also implies that[34]

$$\text{rank}(O(x)) = n \tag{10}$$

with $O(x) = \frac{d\Phi(x)}{dx}$ for all $x \in \Omega_\rho$. Note that the convergence property of the nonlinear observer (8) is obtained based on continuous noise-free output measurements.

Remark 3 *Note that while there are currently no general methods for constructing control Lyapunov functions for general nonlinear systems, significant progress has been made on the constructing control Lyapunov functions for different classes of systems including input affine nonlinear systems*[35] *and constraint linear systems.*[36] *Note also that for broad classes of nonlinear models arising in the context of chemical process control applications, quadratic Lyapunov functions are widely used and provide very good estimates of closed-loop stability regions.*

Robust MHE

The RMHE developed in Ref. 17 is based on an auxiliary nonlinear observer. Specifically, an auxiliary deterministic nonlinear observer that asymptotically tracks the nominal system state is taken advantage of to calculate a confidence region that contains the actual system state taking into account bounded model uncertainties every sampling time. The region is then used to design a constraint on the state estimate in the RMHE. The RMHE brings together deterministic and optimization-based observer design techniques. It was proved to give bounded estimation error in the case of bounded model uncertainties. It was also shown to compensate for the error in the arrival cost approximation and could be used together with different arrival cost approximation techniques to further improve the state estimate. For system (1), the RMHE takes the following form at time instant t_k[17]

$$\min_{\tilde{x}(t_{k-N_e}),\ldots,\tilde{x}(t_k)} \sum_{i=k-N_e}^{k-1} |w(t_i)|^2_{Q_m^{-1}} + \sum_{i=k-N_e}^{k} |v(t_i)|^2_{R_m^{-1}} + V(t_{k-N_e}) \tag{11a}$$

$$\text{s.t. } \dot{\tilde{x}}(t) = f(\tilde{x}(t), u(t), w(t_i)), t \in [t_i, t_{i+1}] \tag{11b}$$

$$v(t_i) = y(t_i) - h(\tilde{x}(t_i)) \tag{11c}$$

$$w(t_i) \in \mathbb{W}, v(t_i) \in \mathbb{V} \tag{11d}$$

$$\dot{z}(t) = F(z(t), u(t), y(t_{k-1})) \tag{11e}$$

$$z(t_{k-1}) = \hat{x}(t_{k-1}) \tag{11f}$$

$$|\tilde{x}(t_k) - z(t_k)| \le \kappa |y(t_k) - h(z(t_k))| \tag{11g}$$

where N_e is the estimation horizon, Q_m and R_m are the estimated covariance matrices of w and v, respectively, $V(t_{k-N_e})$ denotes the arrival cost which summarizes past information up to t_{k-N_e}, $\tilde{x}$ is the predicted x in the above optimization problem, $\hat{x}(t_{k-1})$ is the optimal estimate of x at time

$t_{k-1}, y(t_i)$ is the output measurements at t_i, and κ is a positive constant which is a design parameter. Once optimization problem (11) is solved, an optimal trajectory of the system state, $\tilde{x}^*(t_{k-N}), \ldots, \tilde{x}^*(t_k)$, is obtained. In real-time feedback control applications, only the estimate of the current system state is used. That is

$$\hat{x}(t_k) = \tilde{x}^*(t_k). \tag{12}$$

This is also the case in this work. Note that in the optimization problem (11), w and v are assumed to be piece-wise constant variables with sampling time Δ to ensure that (11) is a finite dimensional optimization problem.

In the optimization problem (11), constraints (11e)–(11g) take advantage of the nonlinear observer F and the previous state estimate to calculate a reference estimate [i.e., $z(t_k)$] of the current state. Based on the reference estimate and the current output measurement [i.e., $y(t_k)$], a confidence region that contains the actual system state is constructed [i.e., $\kappa|y(t_k) - h(z(t_k))|$]. The estimate of the current state provided by the RMHE is only allowed to be optimized within the confidence region. This approach ensures that the RMHE gives estimates with bounded errors and is robust with respect to poor arrival cost approximation. The parameter κ is a design parameter. Theorem 1 below summarizes the properties of RMHE (11).

Theorem 1 *(c.f. Ref.* 17*) Consider system (1) with output* y *sampled at time instants* $\{t_{k\geq 0}\}$. *If RMHE (11) is designed based on nonlinear observer (8) that satisfies condition (9), and if there exists a concave function* $g(\cdot)$ *such that* $g(|e|) \geq \beta(|e|, \Delta)$ *for all* $|e| \leq d_0$ *and positive constants* $d_s < d_0, a \geq 1, b > 0, \epsilon_e > 0$ *such that* $d_s - a(g(d_s) + \gamma_z(\Delta) + \gamma_x(\Delta)) - b\theta_v \geq \epsilon_e$ *where* $\gamma_z(\cdot)$ *and* $\gamma_x(\cdot)$ *are two* $\mathcal{KL}$ *functions depending on the dynamic properties of the nonlinear observer (8), and if the parameter* κ *is picked such that* $0 \leq \kappa \leq \min\{(a-1)/L_h^x, b\}$ *where* L_h^x *is the Lipschitz constant of* $h(x)$, *then the estimation error* $|e| = |\hat{x} - x|$ *is a decreasing sequence such that*

$$|e(t_k)| \leq |e(t_{k-1})| - \epsilon_e \tag{13}$$

for all $d_s \leq |e| \leq d_0$ *and is ultimately bounded as follows*

$$\lim_{t\to\infty} \sup |e(t)| \leq d_{\min} \tag{14}$$

with $d_{\min} = \max\{|e(t+\Delta)| : |e(t)| \leq d_s\}$ *for all* $|e(0)| \leq d_0$.

RMHE-Based LMPC

In this section, the RMHE-LMPC evaluated every sampling time is presented. Specifically, the type of LMPC proposed in Refs. 22 and 23 is considered. The proposed RMHE-LMPC takes into account optimality in both state estimation and control, and bounded model uncertainties explicitly.

LMPC formulation

The proposed RMHE-LMPC uses a standard receding horizon strategy described as follows:

1. At each sampling time t_k, when a new output measurement $y(t_k)$ is received, the RMHE estimates the current system state $\hat{x}(t_k)$ based on current and previous output measurements $y(t_i)$ with $i = k - N_e, \ldots, k$.
2. Based on $\hat{x}(t_k)$, the LMPC calculates future input trajectory $u(t)$ for $t \in [t_k, t_{k+N_c}]$ with N_c the prediction horizon of the LMPC.
3. The LMPC sends the first step input value [i.e., $u(t_k)$] to the actuator.

The design of the LMPC is based on the nominal system model and the state estimate obtained from the RMHE. Specifically, the LMPC is based on the following optimization problem

$$\min_{u\in S(\Delta)} \int_{t_k}^{t_{k+N_c}} \left[|\tilde{x}(\tau)|_{Q_c}^2 + |u(\tau)|_{R_c}^2 \right] d\tau \tag{15a}$$

$$\text{s.t.} \dot{\tilde{x}}(t) = f(\tilde{x}(t), u(t), 0) \tag{15b}$$

$$u \in \mathbb{U} \tag{15c}$$

$$\tilde{x}(t_k) = \hat{x}(t_k) \tag{15d}$$

$$\frac{\partial V(\tilde{x}(t_k))}{\partial \tilde{x}} f(\tilde{x}(t_k), u(t_k), 0) \leq \frac{\partial V(\hat{x}(t_k))}{\partial \hat{x}} f(\hat{x}(t_k), k(\hat{x}(t_k)), 0) \tag{15e}$$

where $S(\Delta)$ is the family of piece-wise constant functions with sampling period Δ, $\tilde{x}(t)$ is the predicted trajectory of the nominal system for the input trajectory computed by the LMPC, and Q_c, R_c are positive definite weighting matrices that define the cost.

In the optimization problem (15), constraint (15a) is the cost function that needs to be minimized; constraint (15b) is the nominal system model governing the evolution of the system state trajectories; constraint (15c) is the constraint on the control input and constraint (15e) is a Lyapunov function based constraint that is used to guarantee the closed-loop stability.

At each sampling time t_k, once an output measurement $y(t_k)$ is received, RMHE (11) is solved to get the current system state estimate $\hat{x}(t_k)$. Based on $\hat{x}(t_k)$, LMPC (15) is solved. The optimal solution to the LMPC is denoted as $u^*(t|t_k)$ which is defined for $t \in [t_k, t_{k+N_c}]$. The control input of system (1) under the control of the RMHE-LMPC is defined as follows

$$u(t) = u^*(t|t_k), \qquad \forall t \in [t_k, t_{k+1}) \tag{16}$$

which implies that the LMPC adopts a standard receding horizon strategy.

The proposed RMHE-based LMPC is different from the LMPC developed in Refs. 22 and 23 in initial condition (15d) and the formulation of the stability constraint (15e). The stability constraint (15e) of the proposed RMHE-LMPC is based on the state estimate given by the RMHE, whereas the stability constraint of the LMPC in Refs. 22 and 23 is based on actual system state. This "slight" modification in the formulation of the LMPC makes the stability results obtained in Refs. 22 and 23 not applicable in the present work. This is because there is in general no separation principles for nonlinear systems. The stability region, stability conditions of the proposed RMHE-LMPC and the interactions between the RMHE and the LMPC need to be carefully studied which are the objectives of the following subsection.

Remark 4 *Constraint (15e) requires that the decreasing rate of the Lyapunov function V if the input of the MPC is used should be greater than or at least equal to the decreasing rate when the auxiliary controller* k *based on the state estimate* $\hat{x}$ *is used. From the property of the RMHE, it is known that the estimation error* $|e| = |\hat{x} - x|$ *is bounded. In order to ensure that the uncertainty in the state estimate will not cause any problem to the stability of the closed-loop system, the proposed approach requires that the initial state of*

the system is within a smaller region compared with the stability region (i.e., Ω_ρ) of the nonlinear controller based on state feedback control. This idea will be made explicit in the next section.

Stability analysis

In this section, we study the robustness of the proposed RMHE-LMPC evaluated every sampling time. Specifically, we first establish the stability region of the closed-loop system under the RMHE-LMPC by taking explicitly into account the state estimation error; then we derive sufficient conditions under which the closed-loop stability of the RMHE-LMPC is guaranteed. The following proposition will be used.

Proposition 1 *(c.f. Ref. 24) Consider the Lyapunov function $V(\cdot)$ of system (1). There exists a $\mathcal{K}$ function $f_V(\cdot)$ such that*

$$V(x) \le V(x') + f_V(|x - x'|) \tag{17}$$

for all $x, x' \in \Omega_\rho$.

Proposition 1 bounds the difference between the magnitudes of two states in the region Ω_ρ which is the stability region of the nonlinear controller $k(x)$ and the LMPC with state feedback. However, because in the proposed RMHE-LMPC, we do not have accurate state feedback and state estimation error is present, the region Ω_ρ is not a good estimate of the stability region of the proposed RMHE-LMPC.

In order to obtain an estimate of the stability region of the RMHE-LMPC, we consider that the initial estimation error $|e(0)| = |x(0) - \hat{x}(0)|$ is bounded by d_0; that is, $|e(0)| \le d_0$. We also assume that $d_{\min} \le d_0$ where $d_{\min}$ is the ultimate upper bound of the estimation error as defined in Theorem 1. From Theorem 1 and the observability assumptions of F, we know that the estimation error is a decreasing sequence and is ultimately bounded by $d_{\min}$ for all $x, \hat{x} \in \Omega_\rho$, which implies that $|e| \le d_0$ for all $x, \hat{x} \in \Omega_\rho$. From Proposition 1, it can be obtained that

$$V(\hat{x}) \le V(x) + f_V(d_0) \tag{18}$$

for all $\hat{x}, x \in \Omega_\rho$. Let us define ρ_e as follows

$$\rho_e = \rho - f_V(d_0). \tag{19}$$

Based on (18) and (19), it can be verified that for any $x \in \Omega_{\rho_e}$ (i.e., $V(x) \le \rho_e$), its estimate given by the RMHE will be in the region Ω_ρ (i.e., $\hat{x} \in \Omega_\rho$). Because of this property, the set Ω_{ρ_e} will be used as an estimate of the stability region of the proposed RMHE-LMPC.

Theorem 2 *Consider system (1) with RMHE (11) and LMPC (15). If $x(0) \in \Omega_{\rho_e}$ and $|\hat{x}(0) - x(0)| \le d_0$, and there exist $\Delta > 0, \epsilon_c > 0, \theta_w > 0$ and $\rho_e > \rho_{\min} > \rho_s > 0$ satisfy*

$$L_V^x M\Delta + L_V^w \theta_w + 2L_V^x d_0 + L_V^u L_k^x d_0 - \alpha_3\left(\alpha_2^{-1}(\rho_s)\right) \le -\epsilon_c/\Delta \tag{20}$$

where L_V^x, L_V^u, L_V^w, and L_k^x are Lipschitz constants associated with $\partial V/\partial x f$ and k(x), then the closed-loop state $x(t) \in \Omega_{\rho_e}$ for all t, and for any k, if $x(t_k) \in \Omega_{\rho_e} \backslash \Omega_{\rho_s}$, the following inequality holds

$$\begin{aligned} &V(x(t_{k+1})) \le V(x(t_k)) - \epsilon_c \\ &V(x(t)) \le V(x(t_k)), \forall t \in [t_k, t_{k+1}] \end{aligned} \tag{21}$$

Furthermore, x(t) is ultimately bounded in $\Omega_{\rho_{\min}} \subset \Omega_{\rho_e}$, that is,

$$\lim_{t \to \infty} \sup V(x(t)) \le \rho_{\min} \tag{22}$$

with $\rho_{\min} = \max\{V(x(t+\Delta)) : V(x) \le \rho_s\}$.

Proof: In this proof, we consider the time derivative of the Lyapunov function V along the state trajectory $x(t)$ in $t \in [t_k, t_{k+1}]$. The time derivative of V is as follows

$$\dot{V}(x(t)) = \frac{\partial V(x(t))}{\partial x} f(x(t), u(t), w(t)). \tag{23}$$

Taking into account constraint (15e), we obtain

$$\begin{aligned} \dot{V}(x(t)) \le{}& \frac{\partial V(x(t))}{\partial x} f(x(t), u(t), w(t)) \\ &+ \frac{\partial V(\hat{x}(t_k))}{\partial x} f(\hat{x}(t_k), k(\hat{x}(t_k)), 0) \\ &- \frac{\partial V(\hat{x}(t_k))}{\partial x} f(\hat{x}(t_k), u(t), 0) \end{aligned} \tag{24}$$

Adding and subtracting $\frac{\partial V(x(t_k))}{\partial x} f(x(t_k), k(x(t_k)), 0)$ to/from the right-hand side of inequality (24), the inequality becomes

$$\begin{aligned} \dot{V}(x(t)) \le{}& \frac{\partial V(x(t))}{\partial x} f(x(t), u(t), w(t)) \\ &- \frac{\partial V(\hat{x}(t_k))}{\partial x} f(\hat{x}(t_k), u(t), 0) \\ &+ \frac{\partial V(\hat{x}(t_k))}{\partial x} f(\hat{x}(t_k), k(\hat{x}(t_k)), 0) \\ &- \frac{\partial V(x(t_k))}{\partial x} f(x(t_k), k(x(t_k)), 0) \\ &+ \frac{\partial V(x(t_k))}{\partial x} f(x(t_k), k(x(t_k)), 0). \end{aligned} \tag{25}$$

From the Lipschitz properties of the function $f(x)$ and the continuous differentiability of $V(x)$, it can be obtained that $\partial V/\partial x f$ is also Lipschitz. The following inequality is obtained

$$\begin{aligned} \dot{V}(x(t)) \le{}& L_V^x |x(t) - \hat{x}(t_k)| + L_V^w |w| + L_V^x |x(t_k) - \hat{x}(t_k)| \\ &+ L_V^u |k(x(t_k)) - k(\hat{x}(t_k))| \\ &+ \frac{\partial V(x(t_k))}{\partial x} f(x(t_k), k(x(t_k)), 0) \end{aligned} \tag{26}$$

where L_V^x, L_V^u, L_V^w are Lipschitz constants of $\partial V/\partial x f$ with respect to its arguments x, u, and w, respectively. Taking into account (6), the boundedness of w and the Lipschitz property of $k(x)$ and applying the results of Theorem 1, the following condition can be obtained for all $x(t) \in \Omega_{\rho_e} \backslash \Omega_{\rho_s}$

$$\dot{V}(x(t)) \le L_V^x |x(t) - \hat{x}(t_k)| + L_V^w \theta_w + L_V^x d_0 + L_V^u L_k^x d_0 - \alpha_3\left(\alpha_2^{-1}(\rho_s)\right) \tag{27}$$

where L_k^x is the Lipschitz constant of k. Using the triangle inequality, $|x(t) - \hat{x}(t_k)|$ can be written as

$$|x(t) - \hat{x}(t_k)| \le |x(t) - x(t_k)| + |x(t_k) - \hat{x}(t_k)|. \tag{28}$$

From the boundedness of u and w, and the Lipschitz property of f, there exists a positive constant M satisfying $|f(x, u, w)| \le M$ for all $x \in \Omega_{\rho_e}$. This implies that

$$|x(t) - x(t_k)| \le M\Delta \tag{29}$$

for $t \in [t_k, t_{k+1}]$. From (28) and (29) and Theorem 1, we get

$$|x(t) - \hat{x}(t_k)| \le M\Delta + d_0 \tag{30}$$

for $t \in [t_k, t_{k+1}]$ and $x \in \Omega_{\rho_e}$. Substituting (30) into (27), we get the following upper bound on the time derivative of Lyapunov function

$$\dot{V}(x(t)) \leq L_V^x M\Delta + L_V^w\theta + 2L_V^x d_0 + L_V^u L_k^x d_0 - \alpha_3\left(\alpha_2^{-1}(\rho_s)\right). \tag{31}$$

If condition (20) is satisfied, then the following inequality holds

$$\dot{V}(x(t)) \leq -\epsilon_c/\Delta. \tag{32}$$

Integrating $\dot{V}(x(t))$ from t_k to t_{k+1}, we obtain inequality (21). Using inequality (21) recursively, if $x(0) \in \Omega_{\rho_e}/\Omega_{\rho_s}$, the state will enter Ω_{ρ_s} in finite sampling steps. Once the state enters $\Omega_{\rho_s} \subset \Omega_{\rho_{\min}}$, it remains inside $\Omega_{\rho_{\min}}$ for all times due to the definition of $\rho_{\min}$. This implies that $x(t)$ is ultimately bounded in $\Omega_{\rho_{\min}}$.

Remark 5 *Figure 1 illustrates the results stated in Theorem 2. When the initial state of the closed-loop system is in Ω_{ρ_e} (i.e., $x(0) \in \Omega_{\rho_e}$), the estimated state may be outside Ω_{ρ_e} but is ensured to be within Ω_ρ (i.e., $\hat{x}(0) \in \Omega_\rho$). As long as the conditions stated in Theorem 2 are satisfied, the value of the Lyapunov function of the actual closed-loop system state is guaranteed to decrease. At the same time, the difference between $\hat{x}$ and x decreases because of the properties of the RMHE. If x is outside Ω_{ρ_s}, the value of the Lyapunov function will continue to decrease; once x enters Ω_{ρ_s}, it may come out of Ω_{ρ_s} but will be within $\Omega_{\rho_{\min}}$.*

Remark 6 *Note that the RMHE based LMPC essentially inherits the stability properties from the observer* F *based nonlinear controller k when implemented in a sample-and-hold fashion in the sense that the observer F based nonlinear controller k provides a worst case solution to the RMHE-based LMPC. However, because the optimality considerations are taken into account in the RMHE-based LMPC, it in general gives a much better closed-loop performance. This point is illustrated in the "Simulation study: application to a chemical process" section.*

RMHE-LMPC with Triggered Implementation

In the previous section, the stability of the RMHE-LMPC evaluated every sampling time was discussed. RMHE and LMPC are both based on solving online optimization problems. For large-scale applications, the computational demand of the RMHE-LMPC may be high. In this section, we propose an RMHE-LMPC design with triggered implementation in order to reduce its computational demand via reducing its total number of observer/controller evaluations. A schematic of the proposed design is shown in Figure 2. In this design, the evaluation of the RMHE-LMPC is triggered by a trigger which is designed based on the differences between the predicted and measured output and output derivatives. Accordingly, to ensure the closed-loop stability, the formulations of the RMHE and the LMPC will be modified to account for possible open-loop operation.

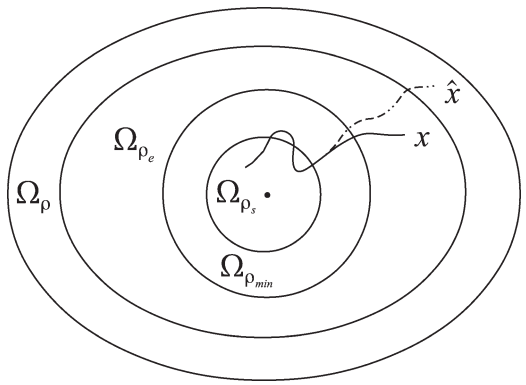

Figure 1. Potential state trajectory (solid line) and estimated state trajectory (dashed line) of the closed-loop system with the proposed RMHE-LMPC that is evaluated at each sampling time.

Triggered Implementation Strategy

The proposed RMHE-LMPC with triggered implementation uses a modified receding horizon strategy in order to reduce the number of observer/controller evaluations. The implementation strategy is as follows:

1. At each sampling time t_k, when a new output measurement $y(t_k)$ is available, the trigger checks the triggering condition. If the triggering condition is satisfied, the trigger sends the current and N_e previous output measurements to the RMHE. The RMHE estimates the current system state $\hat{x}(t_k)$ and go to Step 2. If the triggering condition is not satisfied, go to Step 4.
2. The RMHE sends the current state estimate $\hat{x}(t_k)$ to the LMPC. The LMPC calculates future input trajectory $u(t)$ for $t \in [t_k, t_{k+N_c}]$ based on $\hat{x}(t_k)$.
3. The LMPC sends the entire input trajectory (i.e., $u(t)$ with $t \in [t_k, t_{k+N_c}]$) to the actuator and the predicted future system state trajectory $x^e(t|t_k)$ for $t \in [t_k, t_{k+N_c}]$ to the trigger.
4. Go to Step 1 at the next sampling time t_{k+1}.

Note that in the above triggered implementation strategy, it is assumed that the actuator stores the latest input trajectory sent by the LMPC and keeps implementing the last received input trajectory if no more recent input trajectory is received. The future state trajectory $x^e(t|t_k)$ is the predicted system trajectory according to the input trajectory $u(t)$ for $t \in [t_k, t_{k+N_c}]$ in the LMPC and will be made clear in later discussion. Note that in the triggered implementation strategy, the triggering condition is checked every sampling time. It is possible to check the triggering condition continuously. However, this will require continuous output measurements which may be difficult or expensive to obtain in some applications.

Design of the triggering condition

From the triggered implementation strategy, it can be seen that the triggering condition is checked at sampling instants $\{t_{k\geq 0}\}$ when new system output measurements are available. In the present work, the triggering condition of the RMHE-LMPC is designed based on the differences between the

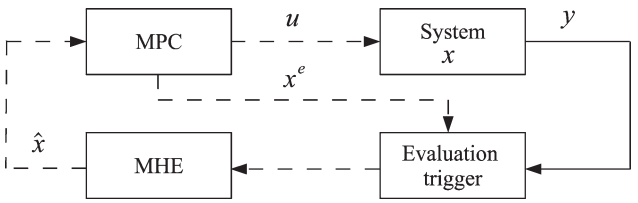

Figure 2. Structure of the proposed RMHE-LMPC with triggered implementation.

predicted and measured output and output time derivatives. Specifically, the triggering condition is designed as follows

$$s(t_k)=\begin{cases}1, & \text{if } |Y(t_k)-Y^e(t_k|t_q)|\geq\epsilon \text{ or } t_k-t_q\geq N_o\Delta\\ 0, & \text{if } |Y(t_k)-Y^e(t_k|t_q)|<\epsilon \text{ and } t_k-t_q<N_o\Delta\end{cases} \tag{33}$$

where Y is the measured output measurement and output time derivatives, $Y^e(t_k|t_q)$ is the predicted output and its time derivatives obtained at t_q which is the last time instant that the RMHE-LMPC was evaluated, ϵ is a predetermined threshold, and N_o is the maximum number of sampling intervals that the RMHE-LMPC is allowed to operate in open-loop. When $s(t_k)=1$, it means that the RMHE-LMPC needs to be re-evaluated; when $s(t_k)=0$, it implies that the triggering condition is not satisfied and the actuator continues to implement the last evaluated control input trajectory. Note that N_o depends on the property of the system and is a design parameter that restricts the maximum open-loop operation time. The value of N_o should be no greater than the prediction horizon of the LMPC N_c in order to guarantee the availability of input trajectory.

We denote the predicted system state trajectory by the LMPC at time t_q as $x^e(t|t_q)$ with $t\in[t_q,t_{q+N_c}]$. This future state trajectory corresponds to the optimal input trajectory calculated by the LMPC at t_q. Based on this predicted state trajectory, predictions of the output trajectory $y^e(t)$ as well as the time derivatives of the output can be calculated. Based on the predicted output $y^e(t|t_q)$ and the output derivatives $y^{e,(r)}(t|t_q)$ $(r=1,\ldots,n-1)$, $Y^e(t|t_q)$ can be constructed. Note that $Y^e=\Phi(x^e)$.

RMHE formulation

Due to the triggered implementation, the system may operate in open-loop for a maximum of N_o sampling intervals. In order to take the potential open-loop operations into account, the RMHE design (11) and the LMPC design (15) need to be modified accordingly to guarantee the closed-loop stability.

In the design of the RMHE, if triggering condition (33) is satisfied at t_k, the nonlinear observer $F(z,u,y)$ is taken advantage of to calculate an estimate of the state at $t_k, z(t_k|t_q)$, based on $\hat{x}(t_q)$ (i.e., the optimal estimate obtained at the last evaluation time t_q) and actual output measurements from t_q to t_k. Based on the estimate $z(t_k|t_q)$ given by the nonlinear observer, a confidence region that contains the actual system state is constructed within which the RMHE optimizes the current state estimate. Specifically, $z(t_k|t_q)$ is calculated based on evaluating the following ordinary differential equations recursively

$$\begin{aligned}\dot{z}(t|t_q)&=F(z(t|t_q),u(t),y(t_{q+l})),\\ &\forall t\in[t_{q+l},t_{q+l+1}),\ l=0,\ldots,N_o-1\end{aligned} \tag{34}$$

with $z(t_q|t_q)=\hat{x}(t_q)$.

Based on $z(t_k|t_q)$, the proposed RMHE accounting for triggered implementation at t_k is designed as follows

$$\min_{\tilde{x}(t_{k-N_e}),\ldots,\tilde{x}(t_k)}\sum_{i=k-N_e}^{k-1}|w(t_i)|^2_{Q_m^{-1}}+\sum_{i=k-N_e}^{k}|v(t_i)|^2_{R_m^{-1}}+V(t_{k-N_e}) \tag{35a}$$

$$\text{s.t. } \dot{\tilde{x}}(t)=f(\tilde{x}(t),u(t),w(t_i)),\ t\in[t_i,t_{i+1}] \tag{35b}$$

$$v(t_i)=y(t_i)-h(\tilde{x}(t_i)) \tag{35c}$$

$$w(t_i)\in\mathbb{W},\ v(t_i)\in\mathbb{V} \tag{35d}$$

$$|\tilde{x}(t_k)-z(t_k|t_q)|\leq\kappa|y(t_k)-h(z(t_k|t_q))| \tag{35e}$$

Besides the difference in the implementation strategies, another important difference between RMHE (35) and RMHE (11) is in the formulation of constraints (11g) and (35e). Specifically, in constraint (35e), $z(t_k|t_q)$ is generated using the deterministic nonlinear observer F starting from $\hat{x}(t_q)$, whereas $z(t_k)$ in constraint (11g) is calculated using the F starting from the previous state estimate $\hat{x}(t_{k-1})$. Once optimization problem (35) is solved, an optimal trajectory of the system states, $\tilde{x}^*(t_{k-N}),\ldots,\tilde{x}^*(t_k)$, is obtained. The optimal estimate of the current system state is defined as

$$\hat{x}(t_k)=\tilde{x}^*(t_k). \tag{36}$$

LMPC formulation

The proposed LMPC accounting for triggered implementation is designed based on the state estimate $\hat{x}(t_k)$ and a nominal sampled trajectory under the control of $k(x)$. Specifically, the nominal sampled trajectory is obtained by integrating the following differential equation recursively

$$\begin{aligned}\dot{x}_n(t|t_k)&=f(x_n(t|t_k),k(x_n(t_{k+l}|t_k)),0),\\ &\forall t\in[t_{k+l},t_{k+l+1}),\ \ l=0,\ldots,N_o-1\end{aligned} \tag{37}$$

with $x_n(t_k|t_k)=\hat{x}(t_k)$. This nominal sampled state trajectory will be used in the design of the LMPC with triggered implementation to formulate a constraint that ensures the closed-loop stability.

Specifically, the LMPC with triggered implementation at an evaluation time t_k is based on the following optimization problem

$$\min_{u\in S(\Delta)}\int_{t_k}^{t_{k+N_c}}\left[|\tilde{x}(\tau)|^2_{Q_c}+|u(\tau)|^2_{R_c}\right]d\tau \tag{38a}$$

$$\text{s.t.}\dot{\tilde{x}}(t)=f(\tilde{x}(t),u(t),0) \tag{38b}$$

$$u\in\mathbb{U} \tag{38c}$$

$$\tilde{x}(t_k)=\hat{x}(t_k) \tag{38d}$$

$$V(\tilde{x}(t))\leq V(x_n(t|t_k)),t\in[t_k,t_{k+N_o}] \tag{38e}$$

where $N_o\leq N_c$. The key difference between the design of LMPC (38) and the design of LMPC (15) is in the Lyapunov function based constraints. Constraint (38e) requires that the stability constraint to be satisfied over the potential maximum open-loop operation time. If we denote the optimal solution given by the above optimization problem as $u_t^*(t|t_k)$ which is defined for $t\in[t_k,t_{k+N_c}]$, the control input of system (1) under the control of the RMHE-LMPC with triggered implementation is determined as follows

$$u(t)=u_t^*(t|t_k),\forall t\in[t_k,t_{k+N_c}). \tag{39}$$

The predicted trajectory [i.e., $\tilde{x}(t)$ in (38)] associated with $u_t^*(t|t_k)$ is defined as $x^e(t|t_k)$ which has been used in the design of the triggering condition.

Stability analysis

The closed-loop stability of the proposed RMHE-LMPC with triggered implementation is analyzed in this section. The following Proposition 2 characterizes the evolution of

the difference between the estimated state given by nonlinear observer (8) and the actual state in one sampling time.

Proposition 2 *(c.f. Ref. 17) Consider observer (8) applied to system (1) with sampled output measurement $y(t_k)$ starting from the initial condition $\hat{x}(t_k)$, the deviation of the observer state z from the actual system state x is bounded for $t \in [t_k, t_{k+1}]$ for $x, \hat{x}, z \in \Omega_\rho$ as follows*

$$|z(t)-x(t)| \leq \beta(|z(t_k)-x(t_k)|, t-t_k)+\gamma_x(t-t_k)+\gamma_z(t-t_k) \tag{40}$$

where $\gamma_z(\cdot)$ and $\gamma_x(\cdot)$ are two $\mathcal{KL}$ functions depending on the dynamic properties of the nonlinear observer (8).

Proposition 3 below provides sufficient conditions under which the estimation error given by RMHE (35) with triggered implementation is a decreasing sequence.

Proposition 3 *Consider system (1) with output y sampled at time instants $\{t_{k\geq 0}\}$. If RMHE (35) is designed based on the nonlinear observer (8) that satisfies condition (9), and if there exists a concave function $g_2(\cdot)$ such that*

$$g_2(|e|) \geq \beta(|e|, \Delta) \tag{41}$$

for all $|e| \leq d_0$ and positive constants $d_{s_2} < d_0, a \geq 1, \epsilon_o > 0$ such that

$$d_{s_2} - a(g_2(d_{s_2})+\gamma_z(\Delta)+\gamma_x(\Delta)+\epsilon_o) \geq 0, \tag{42}$$

and if the parameter κ is picked such that

$$0 \leq \kappa \leq \min\left\{(a-1)/L_h^x, \epsilon_o/\left(\theta_v - L_h^x \epsilon_o\right)\right\} \tag{43}$$

then the estimation error $|e|=|\hat{x}-x|$ is a decreasing sequence for all $d_{s_2} \leq |e| \leq d_0$ and is ultimately bounded as follows

$$\lim_{t\to\infty} \sup |e(t)| \leq d^* \tag{44}$$

with $d^* = \max\{|e(t+\Delta)| : |e(t)| \leq d_{s_2}\}$ for all $|e(0)| \leq d_0$.

Proof: We assume that the last evaluation time of RMHE (35) is t_q. From the formulation of RMHE (35), it can be written that

$$|\hat{x}(t_k) - z(t_k|t_q)| \leq \kappa |y(t_k) - h(z(t_k|t_q))|. \tag{45}$$

From the above inequality and the Lipschitz property of h and the boundedness of the measurement noise, it can be written that

$$|\hat{x}(t_k) - z(t_k|t_q)| \leq \kappa L_h^x |x(t_k) - z(t_k)| + \kappa\theta_v. \tag{46}$$

Using the triangle inequality and from (46), it is obtained that

$$|\hat{x}(t_k) - x(t_k)| \leq \left(\kappa L_h^x + 1\right)|x(t_k) - z(t_k|t_q)| + \kappa\theta_v. \tag{47}$$

From Proposition 2, it can be written that

$$|z(t_k|t_q) - x(t_k)| \leq \beta(|z(t_{k-1}|t_q) - x(t_{k-1})|, \Delta) + \gamma_x(\Delta) + \gamma_z(\Delta). \tag{48}$$

If condition (41) is satisfied, then from the above inequality, it is obtained that

$$|z(t_k|t_q) - x(t_k)| \leq g_2(|z(t_{k-1}|t_q) - x(t_{k-1})|) + \gamma_x(\Delta) + \gamma_z(\Delta) \tag{49}$$

for $|z(t_{k-1}|t_q) - x(t_{k-1})| \leq d_0$. If condition (42) is satisfied, from the above inequality, it is obtained that

$$|z(t_k|t_q) - x(t_k)| \leq \frac{1}{a}|z(t_{k-1}|t_q) - x(t_{k-1})| - \epsilon_o \tag{50}$$

for all $d_{s_2} \leq |z(t_{k-1}|t_q) - x(t_{k-1})| \leq d_0$. Taking into account that $z(t_q|t_q) = \hat{x}(t_q)$ and applying (50) recursively at time instants $t_{q+1}, \ldots, t_k$, it is obtained that

$$|z(t_k|t_q) - x(t_k)| \leq \frac{1}{a^{k-q}}|\hat{x}(t_q) - x(t_q)| - (k-q)\epsilon_o. \tag{51}$$

From (47) and (51) and recalling that $e=|\hat{x}-x|$, it can be written that

$$|e(t_k)| \leq \left(\kappa L_h^x + 1\right)\left(\frac{1}{a^{k-q}}|e(t_q)| - (k-q)\epsilon_o\right) + \kappa\theta_v. \tag{52}$$

If κ is picked following (43), then it can be obtained from the above inequality that

$$|e(t_k)| \leq |e(t_q)| - \epsilon_{e_2} \tag{53}$$

for $d_{s_2} \leq |e| \leq d$. This implies that $|e|$ decreases at two consecutive evaluation times of RMHE (35) and will become smaller than d_{s_2} in finite steps. Once $|e| < d_{s_2}$, it will remain to satisfy $|e(t)| \leq d^*$ due to the definition of d^* and the design of the RMHE. This implies that

$$\lim_{t\to\infty} \sup |e(t)| \leq d^*. \tag{54}$$

This proves Proposition 3.

Proposition 4 below summarizes the stability properties of the nonlinear controller $k(x)$ with sample-and-hold implementation.

Proposition 4 *(c.f. Ref. 26) Consider the nominal sampled trajectory $x_n(t)$ of system (1) in closed-loop for a controller $k(x)$ as defined in (37). Let $\Delta, \epsilon_s > 0$ and $\rho > \rho_s > 0$ satisfy*

$$-\alpha_3(\alpha_2^{-1}(\rho_s)) + L_V^x M \Delta \leq -\epsilon_s/\Delta. \tag{55}$$

Then, if $\rho_{\min} < \rho$ where $\rho_{\min} = \max\{V(x(t+\Delta)) : V(x(t)) \leq \rho_s\}$ and $x_n(0) \in \Omega_\rho$, the following inequality holds

$$V(x_n(t)) \leq V(x_n(t_k)), \forall t \in [t_k, t_{k+1}), \tag{56}$$

$$V(x_n(t_k)) \leq \max\{V(x_n(0)) - k\epsilon_s, \rho_{\min}\}. \tag{57}$$

Based on the above propositions, the following Theorem 3 summarizes the stability properties of the RMHE-LMPC with triggered implementation.

Theorem 3 *Consider system (1) with RMHE (35) and LMPC (38) with triggered implementation and the triggered condition (33). If $x(0) \in \Omega_{\rho_e}$ and $|\hat{x}(0) - x(0)| \leq d_0$, and there exist $\Delta > 0, \epsilon > 0, \epsilon_s > 0, \theta_w > 0, \theta_\phi > 0$ and $\rho_e > \rho^* > \rho_{s,2} > 0$ satisfy*

$$\begin{aligned} &-\epsilon_s + f_V\left(\left(L_\Phi \epsilon + L_\Phi \theta_\phi + L_f^v \theta_w / L_f^x\right) e^{L_f^x \Delta} - L_f^v \theta_w / L_f^x\right) \\ &\quad + f_V(d_0) < 0, \end{aligned} \tag{58}$$

then the closed-loop state $x(t) \in \Omega_{\rho_e}$ for all t and $x(t)$ is ultimately bounded in $\Omega_{\rho^*} \subset \Omega_{\rho_e}$, that is,

$$\lim_{t\to\infty} \sup V(x(t)) \leq \rho^* \tag{59}$$

with $\rho^* = \rho_{\min} + f_V\left(\left(L_\Phi \epsilon + L_\Phi \theta_\phi + L_f^v\ \theta_w / L_f^x\right) e^{L_f^x \Delta} - L_f^v \theta_w / L_f^x\right) + f_V(d_0)$.

Proof: In this proof, we assume that the last evaluation time of the RMHE-LMPC is t_q and that the triggering condition is satisfied right after t_{k-1} $(t_{k-1} > t_q)$ and the RMHE-

LMPC is re-evaluated at t_k. This scenario corresponds to the worst case scenario of the triggered implementation. This worst scenario implies that

$$|Y(t_{k-1}) - Y^e(t_{k-1}|t_q)| = \epsilon. \tag{60}$$

From constraint (38e), it can be written that

$$V(x^e(t|t_q)) \le V(x_n(t|t_q)) \tag{61}$$

for $t \in [t_q, t_{q+N_o}]$. From Proposition 4, it can be obtained that

$$V(x_n(t_k|t_q)) \le \max\{V(x_n(t_q|t_q)) - (k-q)\epsilon_s, \rho_{\min}\} \tag{62}$$

for $x_n(t_k|t_q) \in \Omega_\rho$. From inequalities (61) to (62) and the fact that $x^e(t_q|t_q) = x_n(t_q|t_q)$, the following inequality can be obtained

$$V(x^e(t_k|t_q)) \le \max\{V(x^e(t_q|t_q)) - (k-q)\epsilon_s, \rho_{\min}\} \tag{63}$$

for $x^e(t_q|t_q) \in \Omega_\rho$. From Proposition 1, it can be written that

$$V(x(t_k)) \le V(x^e(t_k|t_q)) + f_V(|x(t_k) - x^e(t_k|t_q)|) \tag{64}$$

From inequalities (63) to (64), it is obtained that

$$V(x(t_k)) \le \max\{V(x^e(t_q|t_q)) - (k-q)\epsilon_s, \rho_{\min}\} + f_V(|x(t_k) - x^e(t_k|t_q)|). \tag{65}$$

Note that from the observability assumption (i.e., $\text{rank}(O(x)) = n$) and implicit function theorem, $\Phi(x)$ is invertible for $x \in \Omega_\rho$. Noticing that $\Phi(x^e) = Y^e$ and $\Phi(x) = Y - \phi$ (from its definition), it can be written that

$$|x^e(t_{k-1}|t_q) - x(t_{k-1})| = |\Phi^{-1}(Y^e(t_{k-1}|t_q) - \Phi^{-1}(Y(t_{k-1}) - \phi(t_{k-1}))|. \tag{66}$$

From (66) and the Lipschitz property of Φ^{-1}, the following inequality can be derived

$$|x^e(t_{k-1}|t_q) - x(t_{k-1})| \le L_\Phi |Y^e(t_{k-1}|t_q) - Y(t_{k-1}) + \phi(t_{k+1})|. \tag{67}$$

From (60), (67) and the boundedness of $\phi(t)$, it can be obtained that

$$|x^e(t_{k-1}|t_q) - x(t_{k-1})| \le L_\Phi \epsilon + L_\Phi \theta_\phi. \tag{68}$$

From the definition of $x^e(t|t_q)$ and the system model, it can be written that

$$|\dot{x}^e(t|t_q) - \dot{x}(t)| = |f(x^e(t|t_q), u(t), 0) - f(x(t), u(t), w(t))|. \tag{69}$$

Based on the Lipschitz property of f, it is obtained that

$$|\dot{x}^e(t|t_q) - \dot{x}(t)| \le L_f^x |x^e(t|t_q) - x(t)| + L_f^v \theta_w. \tag{70}$$

Integrating Eq. 70 from t_{k-1} to t_k and using condition (68), it is obtained that

$$|x^e(t_k|t_q) - x(t_k)| \le \left(L_\Phi \epsilon + L_\Phi \theta_\phi + L_f^v \theta_w / L_f^x\right) e^{L_f^x \Delta} - L_f^v \theta_w / L_f^x. \tag{71}$$

From (65) and (71), it can be obtained that

$$V(x(t_k)) \le \max\{V(x^e(t_q|t_q)) - (k-q)\epsilon_s, \rho_{\min}\} + f_V\left(\left(L_\Phi \epsilon + L_\Phi \theta_\phi + L_f^v \theta_w / L_f^x\right) e^{L_f^x \Delta} - L_f^v \theta_w / L_f^x\right). \tag{72}$$

From Proposition 3 and recalling that $x^e(t_q|t_q) = \hat{x}(t_q)$, it can be written that

$$|x^e(t_q|t_q) - x(t_q)| \le d_0 - c\epsilon_{e_2} \tag{73}$$

where c is the number of evaluations of the RMHE-LMPC until t_q. From (72) to (73), and applying Proposition 1, the following inequality can be obtained

$$V(x(t_k)) \le \max\{V(x(t_q)) - (k-q)\epsilon_s, \rho_{\min}\} + f_V\left(\left(L_\Phi \epsilon + L_\Phi \theta_\phi + L_f^v \theta_w / L_f^x\right) e^{L_f^x \Delta} - L_f^v \theta_w / L_f^x\right) + f_V(d_0 - c\epsilon_{e_2}). \tag{74}$$

If condition (58) holds, there exists a positive $\epsilon_c > 0$ such that the following inequality is satisfied for any $k - q \ge 1$ and $c \ge 1$

$$V(x(t_k)) \le \max\{V(x(t_q)) - \epsilon_c, \rho^*\} \tag{75}$$

for all $x \in \Omega_{\rho_e}$. Using inequality (75) recursively, if $x_0 \in \Omega_{\rho_e} / \Omega_{\rho_{s,2}}$, the state will enter $\Omega_{\rho_{s,2}}$ in finite sampling steps. Once the state enters $\Omega_{\rho_{s,2}} \subset \Omega_{\rho^*}$, it remains inside Ω_{ρ^*} for all times due to the definition of ρ^*. This implies that $x(t)$ is ultimately bounded in Ω_{ρ^*}.

Remark 7 *Referring to condition (58) in Theorem 3, the second term of the left-hand-side characterizes the effect of uncertainties in measurements and the triggering design on the evolution of the Lyapunov function; the third term of the left-hand-side characterizes the effect of the estimation error on the evolution of the Lyapunov function. Note that condition (58) could be conservative as the worst case scenario is considered in the derivation of the results.*

Remark 8 *The conditions provided in Theorem 1 and Theorem 3 provide insights into the interplay between the different parameters. These conditions can be used as guidelines to tune the parameter κ and ϵ. However, it may be conservative to calculate κ and ϵ based on these conditions as they are derived based on the worst case scenarios. In practice, these parameters could be tuned via offline simulations. For a detailed discussion on how to tune κ via simulations, the reader is referred to Ref. 17. Regarding the estimation of the most appropriate ϵ for the triggered implementation, it can be done by simulating the process with different values of ϵ to obtain the dependency of the performance and evaluation numbers on ϵ. The most appropriate ϵ would be a tradeoff between performance and evaluation time. Please see the "Simulation study: application to a chemical process" section for an application of this approach.*

Simulation Study: Application to a Chemical Process

Process description and modeling

In this section, the proposed RMHE-LMPC and its triggering implementation will be applied to a chemical process composed of two connected continuous-stirred tank reactors (CSTR) as shown in Figure 3. Similar processes have been studied in Refs. 37 and 38 in the context of networked process control and fault-tolerant control. The feed stream entering the first tank contains pure reactant A at flow rate F_0, molar concentration C_{A0} and temperature T_0. Three parallel irreversible exothermal reactions take place in the reactor: $A \to B, A \to C$, and $A \to D$, where B is the product, and C and D are byproducts. The effluent of CSTR 1 is fed into

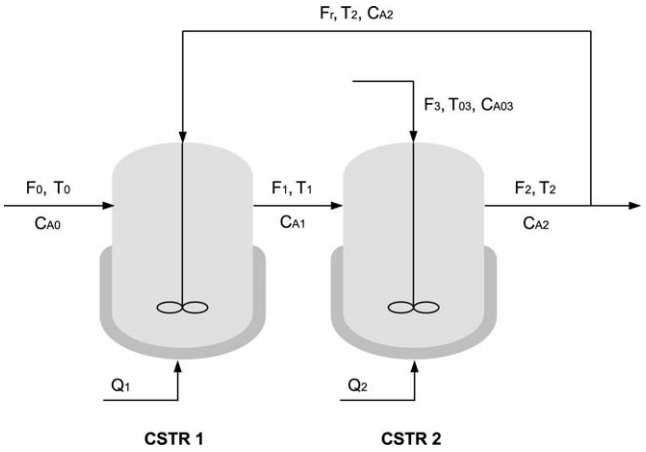

Figure 3. Two connected CSTRs with recycle stream.

CSTR 2 at flow rate F_1, molar concentration C_{A1}, and temperature T_1. There is also another flow of pure A that is fed into CSTR 2 at flow rate F_3, molar concentration C_{A03}, and temperature T_{03}. The same reactions take place in CSTR 2. A portion of the effluent of CSTR 2 is passed through a separator and recycled back to CSTR 1 with unreacted A at recycle flow rate F_r, molar concentration C_{A2}, and temperature T_2. Each reactor is equipped with a jacket to provide/remove heat to/from the reactor. Based on standard modeling assumptions and mass and energy balances, four ordinary differential equations can be obtained to describe the dynamics of the process

$$\begin{aligned}
\frac{dT_1}{dt} &= \frac{F_0}{V_1}(T_0-T_1)+\frac{F_r}{V_1}(T_2-T_1)-\sum_{i=1}^{3}\frac{\Delta H_i}{\rho c_p}k_{i0}e^{\frac{-E_i}{RT_1}}C_{A1}+\frac{Q_1}{\rho c_p V_1}\\
\frac{dC_{A1}}{dt} &= \frac{F_0}{V_1}(C_{A0}-C_{A1})+\frac{F_r}{V_1}(C_{A2}-C_{A1})-\sum_{i=1}^{3}k_{i0}e^{\frac{-E_i}{RT_1}}C_{A1}\\
\frac{dT_2}{dt} &= \frac{F_1}{V_2}(T_1-T_2)+\frac{F_3}{V_2}(T_{03}-T_2)-\sum_{i=1}^{3}\frac{\Delta H_i}{\rho c_p}k_{i0}e^{\frac{-E_i}{RT_2}}C_{A2}+\frac{Q_2}{\rho c_p V_2}\\
\frac{dC_{A2}}{dt} &= \frac{F_1}{V_2}(C_{A1}-C_{A2})+\frac{F_3}{V_2}(C_{A03}-C_{A2})-\sum_{i=1}^{3}k_{i0}e^{\frac{-E_i}{RT_2}}C_{A2}
\end{aligned} \tag{76}$$

where $T_j, C_{Aj}, Q_j, V_j, j=1,2$ denote the temperature of in the reactors, the concentration of A, the rate of the heat input/removal to/from the reactors and the reactor volumes, respectively, c_p and ρ denote the heat capacity and density of the mixture in the reactors, $\Delta H_i, k_i, E_i, i=1,2,3$ denote the enthalpies, pre-exponential constants, and activation energies of the reactions, respectively. The values of these parameters are given in Table 1.

It is assumed that the measured outputs of the process are the two temperatures (i.e., T_1 and T_2) and the measurements are subject to bounded noise. The bounded noise in the measurements is generated as normal distributed values with zero mean and standard deviation 1 but the values are restricted to be in the interval $[-1,1]$. In addition to the measurement noise, bounded random disturbances are added to the right-hand-side of Eq. 76. The random disturbance added to the dynamics of the temperatures is generated as normal distributed values with zero mean and standard deviation 1 in the range $[-1,1]$, whereas the disturbance added to the dynamics of the concentrations is generated as normal distributed values with zero mean and standard deviation 0.1 in the range $[-0.5,0.5]$. The rate of heat input/removal to/from the two reactors, Q_1 and Q_2, are the control inputs of the process. The control inputs are subject to the constraint $|Q_i| \le 10^6$ kJ $/h (i=1,2)$. The process has two stable steady-states and one unstable steady-state. The unstable steady-state is

$$\begin{aligned}
x_s &= \left[T_1^s\ C_{A1}^s\ T_2^s\ C_{A2}^s\right]^T\\
&= \left[457.943\ \text{K}\ 1.770\ \text{kmol/m}^3\ 415.459\ \text{K}\ 1.752\ \text{kmol/m}^3\right]^T
\end{aligned} \tag{77}$$

which is the desired operating point.

Table 1. Process Parameters for the Reactors

$F_0=4.998\text{m}^3/\text{h}$	$\Delta H_1=-5.0\times10^4\text{KJ/kmol}$
$F_1=39.996\text{m}^3/\text{h}$	$\Delta H_2=-5.2\times10^4\text{KJ/kmol}$
$F_3=30.0\text{m}^3/\text{h}$	$\Delta H_3=-5.04\times10^4\text{KJ/kmol}$
$V_1=1.0\text{m}^3/\text{h}$	$k_{10}=3.0\times10^6\text{h}^{-1}$
$V_2=3.0\text{m}^3/\text{h}$	$k_{20}=3.0\times10^5\text{h}^{-1}$
$R=8.314\text{KJ/kmol}\cdot\text{K}$	$k_{30}=3.0\times10^5\text{h}^{-1}$
$T_0=300\text{K}$	$E_1=5.0\times10^4\text{KJ/kmol}$
$T_{03}=300\text{K}$	$E_2=7.53\times10^4\text{KJ/kmol}$
$C_{A0}=4.0\text{kmol/m}^3$	$E_3=7.53\times10^4\text{KJ/kmol}$
$C_{A03}=2.0\text{kmol/m}^3$	$\rho=1000.0\text{kg/m}^3$
$c_p=0.231\text{KJ/kg}$	

Observer and controller designs

Process (76) belongs to the following class of nonlinear systems

$$\begin{aligned}
\dot{x}(t) &= f(x(t))+g(x(t))u(t)\\
y(t) &= Cx(t)
\end{aligned} \tag{78}$$

where $x=[x_1\,x_2\,x_3\,x_4]^T=\left[T_1-T_1^s\ C_{A1}-C_{A1}^s\ T_2-T_2^s\ C_{A2}-C_{A2}^s\right]^T$ is the state vector, $u=[u_1\,u_2]^T=[Q_1\,Q_2]^T$ is the input vector, $y=[y_1\,y_2]^T=[T_1\,T_2]^T$ is the output vector, f is a 4 by 1 vector function, g is a 4 by 2 matrix function, and $C=\begin{bmatrix}1&0&0&0\\0&0&1&0\end{bmatrix}$.

First, a deterministic nonlinear observer is designed following Ref. 39 for process (76) to estimate the process state based on the two temperature measurements. The nonlinear observer takes the following form

$$\dot{\hat{x}}(t)=f(\hat{x}(t))+g(\hat{x}(t))u(t)+G(\hat{x}(t))^{-1}K(y(t)-C\hat{x}(t)) \tag{79}$$

where $\hat{x}$ denotes the state of the observer and

$$\begin{aligned}
G&=\begin{bmatrix}G_1&0\\0&G_2\end{bmatrix},\quad G_1=\begin{bmatrix}1&0\\\dfrac{\partial f_1}{\partial T_1}&\dfrac{\partial f_1}{\partial C_{A1}}\end{bmatrix},\\
G_2&=\begin{bmatrix}1&0\\\dfrac{\partial f_3}{\partial T_2}&\dfrac{\partial f_3}{\partial C_{A2}}\end{bmatrix}
\end{aligned} \tag{80}$$

with f_1 and f_3 the first and third elements in the vector function f, respectively. In observer (79), $K=\left[K_1^T K_2^T\right]^T$ is a gain matrix. In this example, $K_1=K_2=K_o$ and their values are

determined such that the eigenvalues of the matrix $A_o - K_o C_o$ with $A_o = \begin{bmatrix} 0 & 1 \\ 0 & 0 \end{bmatrix}$ and $C_o = [1\ 0]$ are placed at $-20 \pm i$. This nonlinear observer can asymptotically track the state of the nominal process of Eq. (76).

Second, a state feedback nonlinear controller is designed via feedback linearization to manipulate the control inputs as follows[33]

$$\begin{aligned} u_1(t) &= -\rho c_p V_1 (f_1(x(t)) + K_{c1} x_1) \\ u_2(t) &= -\rho c_p V_2 (f_3(x(t)) + K_{c2} x_3) \end{aligned} \tag{81}$$

where K_{c1} and K_{c2} are two tuning parameters. In this example, the two parameters are tuned to be $K_{c1} = K_{c2} = 5$. This nonlinear controller can asymptotically stabilize the closed-loop nominal process of Eq. (76) at the desired steady state x_s.

On the basis of the nonlinear observer (79), we design the RMHE and based on the nonlinear controller (81), we design the LMPC. In the designs, the sampling time is $\Delta = 0.01h$. In order to account for different orders of magnitude of the state values, constraints (11g) and (35e) are decomposed into four constraints as follows

$$\begin{aligned} |\tilde{T}_1(t_k) - z_1(t_k)| &\le \kappa_1 |y(t_k) - h(z(t_k))| \\ |\tilde{C}_{A_1}(t_k) - z_2(t_k)| &\le \kappa_2 |y(t_k) - h(z(t_k))| \\ |\tilde{T}_2(t_k) - z_3(t_k)| &\le \kappa_1 |y(t_k) - h(z(t_k))| \\ |\tilde{C}_{A_2}(t_k) - z_4(t_k)| &\le \kappa_2 |y(t_k) - h(z(t_k))| \end{aligned} \tag{82}$$

with $\kappa_1 = 1, \kappa_2 = 0.1$, and $z_1(t_k), z_2(t_k), z_3(t_k)$, and $z_4(t_k)$ the four elements of $z(t_k)$. These parameters are designed based on extensive offline simulations when considering the range difference between temperature and concentration. A quadratic Lyapunov function $V(x) = x^T P x$ is considered with $P = \text{diag}([1\ 100\ 1\ 50])$. The weighting matrices in the cost function of the RMHE are $Q_m = \text{diag}([1\ 0.01\ 1\ 0.01])$ and $R_m = \text{diag}([1\ 1])$. The weighting matrices in the cost function of the LMPC are $Q_c = \text{diag}([1\ 100\ 1\ 50])$ and $R_c = \text{diag}([10^{-8} 10^{-8}])$. In Section, the performance of the proposed RMHE-LMPC will be compared with a classical MHE-based LMPC. The classical MHE (e.g., Ref. 9) is designed based on the same parameters as used in the RMHE. Both of the RMHE and the classical MHE use the extended Kalman filtering approach to approximate the arrival cost.[13]

RMHE-LMPC evaluated every sampling time

In this section, the performance of three different control strategies will be compared. Specifically, the three control strategies are: (1) the proposed RMHE-LMPC, (2) the classical MHE-based LMPC, and (3) the nonlinear controller (81) based on the nonlinear observer (79) implemented in a sample-and-hold fashion. In the simulations, these controllers are evaluated every Δ; the estimation horizon of the RMHE and MHE is $N_e = 3$; and the prediction horizon of the LMPC is $N_c = 3$.

Figure 4 shows the trajectories of the states of process (76) under the three control strategies for a simulation duration $t_f = 1.0\,h$. In this set of simulations, the initial condition of the process is $x(0) = [453.943\,\text{K},\ 1.570\,\text{kmol/m}^3,\ 410.959\,\text{K},\ 1.552\,\text{kmol/m}^3]^T$ and the initial guess used in the observers is $\hat{x}_0 = [453.923\,\text{K},\ 1.568\,\text{kmol/m}^3,\ 410.039\,\text{K},\ 1.550\,\text{kmol/m}^3]^T$. From Figure 4, it can be seen that both the proposed RMHE-LMPC and the classical MHE-based

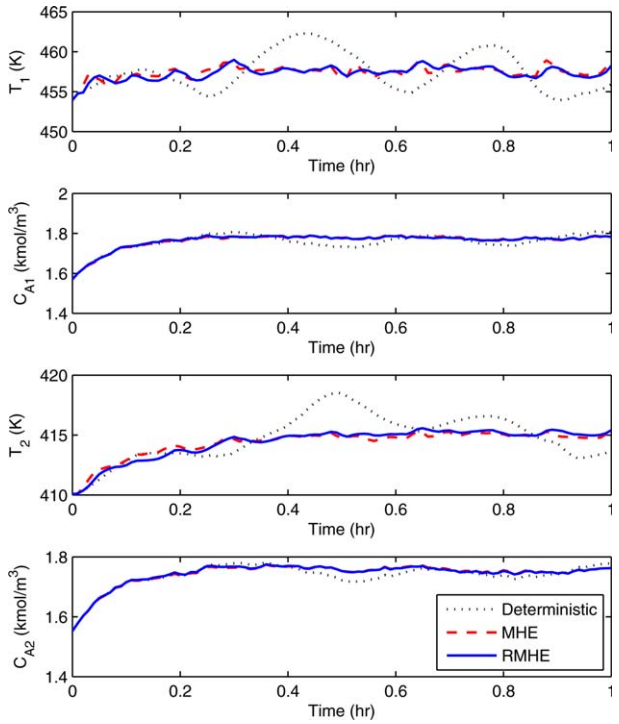

Figure 4. State trajectories of process (76) under the proposed RMHE-LMPC evaluated every sampling time (solid lines), the classical MHE-based LMPC (dashed lines) and the nonlinear observer (79)-based nonlinear controller (81) implemented in a sample-and-hold fashion (dotted lines).

[Color figure can be viewed in the online issue, which is available at wileyonlinelibrary.com.]

LMPC can drive the process state to a small region around the operating steady-state. It can also be seen that trajectories obtained under the observer (79)-based controller (81) exhibit relatively large oscillations around the steady-state values. This reveals a very interesting property of the proposed RMHE-LMPC. That is, even the proposed RMHE-LMPC is designed based on the nonlinear observer (79) and nonlinear controller (81), it gives a much better performance than observer (79)-based controller (81).

Before proceeding to the comparison of the control performance of the proposed RMHE-LMPC and the classical MHE-based LMPC, we carried out a set of simulations to compare the performance of the RMHE and the classical MHE from the boundedness of state estimation error point of view. In this set of simulations, the initial process state and the initial observer guess are chosen to be the same as

$$\begin{aligned} x(0) &= \hat{x}(0) \\ &= [458.143\,\text{K}\ 1.780\,\text{kmol/m}^3\ 415.729\,\text{K}\ 1.762\,\text{kmol/m}^3]^T \end{aligned} \tag{83}$$

which is close to the operating steady-state. The selection of the initial state and initial guess is to eliminate the effects of process and observer transients and to focus on the ultimate boundedness of the estimation error. The simulation duration is $t_f = 5.0\,h$, which is sufficiently long to reflect the randomness of process disturbances and measurement noise. To account for the different magnitudes of the estimation errors

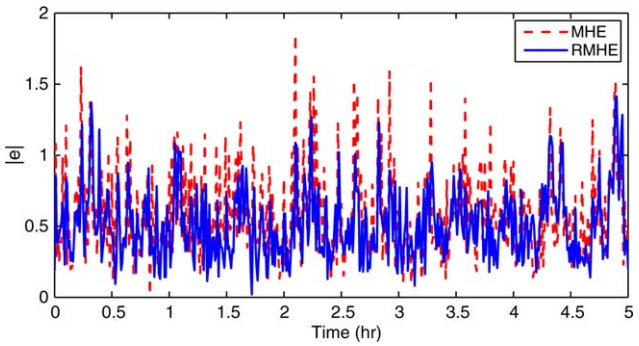

Figure 5. Normalized norm of the estimation errors of the RMHE (solid lines) and the classical MHE (dashed lines).

[Color figure can be viewed in the online issue, which is available at wileyonlinelibrary.com]

for different states, the error for each state is normalized based on its maximum estimation error as in Ref. 16. Figure 5 shows the Euclidean norm of the normalized estimation errors given by the RMHE and the classical MHE. The maximum estimation errors given by the RMHE and the classical MHE are 1.4145 and 1.8521, respectively. The averages and standard deviations of the normalized estimation errors over the simulation time are also calculated. For the RMHE, the average is 0.5100 and the standard deviation is 0.2486. For the classical MHE, the average is 0.5819 and the standard deviation is 0.3068. These results show that the RMHE gives a better estimation performance compared with the classical MHE.

We also carried out a set of simulations to compare the overall control performance of the proposed RMHE-LMPC and the classical MHE-based LMPC from a performance index point of view based on the following performance index

$$J=\sum_{k=0}^{M}\left[|x(t_k)|^2_{Q_c}+|u(t_k)|^2_{R_c}\right] \tag{84}$$

where $t_0=0$ is the initial simulation time and $t_M=1.0\,h$ is the end of simulation time. Note that the parameters Q_c and R_c in (84) are the same as those in the MPC objective function. The process and the observers are initialized with different initial states and initial guesses. Different random sequences for the process disturbances and measurement noise are used for different simulation runs. Table 2 shows the simulation results for 13 simulation runs. From the table, it can be seen that the proposed RMHE-LMPC gives the best performance in all of the 13 simulations and observer (79)-based controller (81) gives the worst performance. The proposed RMHE-LMPC gives a better performance than the classical MHE-based LMPC because the RMHE in general provides better state estimates due to the confidence region information provided by the nonlinear observer (79) at each sampling time.

RMHE-LMPC with triggered implementation

In this section, the control performance and evaluation times of the proposed RMHE-LMPC with triggered implementation is studied under different triggering thresholds (i.e., ϵ). In the simulations, the estimation horizon is $N_e=3$ and the prediction horizon is $N_c=3$. As explained in Remark 2, as we have two temperature outputs in this example, in the design of the triggering condition, only the first-order time derivatives of the two temperatures are needed in order to have a full rank observability matrix. Specifically, in the design of the triggering condition

$$Y(t_k)=[T_1(t_k)\;T_1(t_k)-T_1(t_{k-1})\;T_2(t_k)\;T_2(t_k)-T_2(t_{k-1})]^T \tag{85}$$

where the changes of $T_i, i=1,2$, over one sampling interval are used to approximate the first-order time derivatives of $T_i, i=1,2$. The predicted Y^e is calculated similarly. The design parameter N_o is picked to be 3 so that $N_o \leq N_c$.

Figure 6 shows the closed-loop state trajectories of process (76) when the triggering condition threshold $\epsilon=0.8$. From Figure 6, it can be seen that the proposed triggered implementation of the RMHE-based LMPC is able to drive the state of the closed-loop system to a small region around the desired steady state.

We also carried out simulations to compare the RMHE-LMPC with triggered implementation and the RMHE-LMPC evaluated every sampling time in terms of performance and number of controller evaluations. Specifically, simulations were conducted under different settings (noise upper bounds, initial conditions, triggering thresholds) and the average performance and evaluation times were calculated with respect to the threshold ϵ. For each triggering threshold, 10 simulation runs were used to calculate the average performance cost and the evaluation times. Figure 7 shows the simulation results. From the bottom plot in Figure 7, we can see that the performance index increases as the value of the threshold ϵ increases. However, when ϵ is sufficiently small (e.g., $\epsilon \leq 1$), the performance index given by the RMHE-LMPC with triggered implementation is very close to the one given by the RMHE-LMPC evaluated every sampling time. From the top plot in Figure 7, it can be seen that the evaluation times of the RMHE-LMPC decreases dramatically with the increase of the threshold ϵ. This set of simulations demonstrates that the triggered implementation can reduce the computational burden of the RMHE-LMPC and maintain the performance close to the one obtained by the RMHE-LMPC evaluated every sampling time if a proper triggering threshold is used.

Table 2. Performance Comparison. Performance given by (1) observer (79) based controller (81), (2) the classical MHE based LMPC, and (3) the proposed RMHE-LMPC

	(1)	(2)	(3)
1	405.4987	299.5536	201.2114
2	799.4618	778.9133	643.2531
3	1625.7000	1058.0000	818.7161
4	2763.3000	2008.3000	1967.8000
5	2966.7000	1458.8000	1320.4000
6	779.8802	481.8757	474.8328
7	1335.5000	626.8311	594.7462
8	2295.8000	631.8616	594.3354
9	883.1589	584.9754	568.3884
10	833.1237	777.0954	644.7041
11	1234.8000	625.2982	585.8234
12	793.7693	563.7527	534.9076
13	2155.3000	2018.9000	1914.0000

Performance given by (1) observer (79) based controller (81), (2) the classical MHE based LMPC, and (3) the proposed RMHE-LMPC.

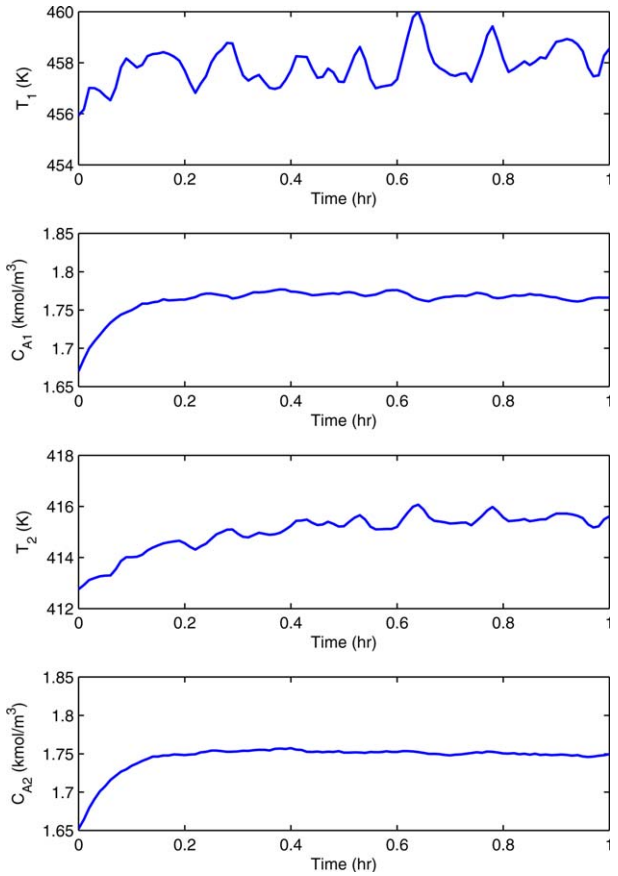

Figure 6. State trajectories of process (76) under the proposed RMHE-LMPC with triggered implementation with ϵ=0.8.

[Color figure can be viewed in the online issue, which is available at wileyonlinelibrary.com.]

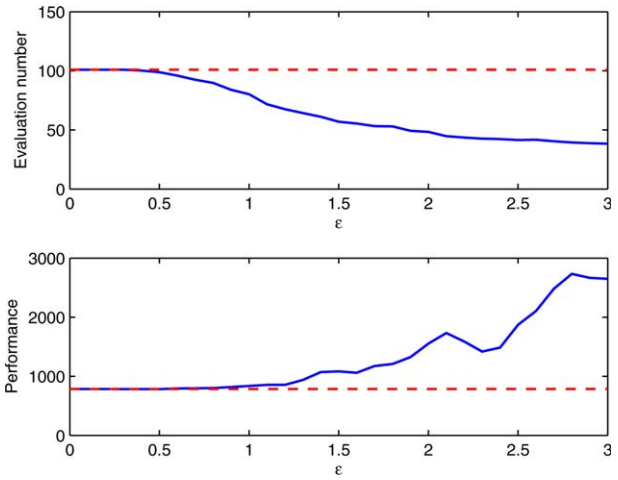

Figure 7. Average evaluation time and performance index of the RMHE-LMPC with triggered implementation with the triggering thresholds varying from 0 to 2 (solid lines). The dashed line indicate the performance of the RMHE-LMPC evaluated every sampling time.

[Color figure can be viewed in the online issue, which is available at wileyonlinelibrary.com.]

Conclusions

In this work, the robustness properties of RMHE-LMPC for nonlinear systems with bounded uncertainties with both every-sampling-time evaluation and triggered evaluation were studied. Specifically, in the first part, we considered the RMHE-LMPC evaluated every sampling time. In this case, an estimate of the stability region of the output feedback control system taking into account estimation error explicitly was first established; and then sufficient conditions under which the closed-loop system with the output feedback control system is guaranteed to be stable were derived. In order to reduce the computational load of the RMHE-LMPC, a triggered implementation strategy was proposed in the second part. The triggering condition was designed based on the measurements of the output and its time derivatives. In order to ensure the closed-loop stability, the formulations of the RMHE and the LMPC were also modified accordingly to account for the potential open-loop operation time. Sufficient conditions for stability of the closed-loop system were also derived. The applicability and effectiveness of the proposed RMHE-LMPC designs were illustrated via the application to a chemical process.

Literature Cited

1. Mayne DQ, Rawlings JB, Rao CV, Scokaert POM. Constrained model predictive control: stability and optimality. *Automatica*. 2000; 36:789–814.
2. Findeisen R, Imsland L, Allgöwer F, Foss BA. Output feedback stabilization of constrained systems with nonlinear predictive control. *Int J Robust Nonlin Control*. 2003;13:211–227.
3. Heidarinejad M, Liu J, Christofides PD. State estimation-based economic model predictive control of nonlinear systems. *Syst Control Lett*. 2012;61:926–935.
4. Wan Z, Kothare WV. Efficient scheduled stabilizing model predictive control for constrained nonlinear systems. *Int J Robust Nonlin Control*. 2003;13:331–346.
5. Bemporad A, Garulli A. Output-feedback predictive control of constrained linear systems via set membership state estimation. *Int J Cotnrol*. 2000;73:655–665.
6. Cannon M, Cheng Q, Kouvaritakis B, Rakovic SV. Stochastic tube MPC with state estimation. *Automatica*. 2012;48:536–541.
7. Findeisen R, Imsland L, Allgöwer F, Foss BA. State and output feedback nonlinear model predictive control: an overview. *Eur J Control*. 2003;9:190–206.
8. Rao CV, Rawlings JB, Lee JH. Constrained linear state estimation-a moving horizon approach. *Automatica*. 2001;37:1619–1628.
9. Rao CV, Rawlings JB, Mayne DQ. Constrained state estimation for nonlinear discrete-time systems: stability and moving horizon approximations. *IEEE Trans Autom Control*. 2003;48:246–258.
10. Rawlings JB, Ji L. Optimization-based state estimation: current status and some new results. *J Process Control*. 2012;22:1439–1444.
11. Huang R, Biegler LT, Patwardhan SC. Fast offset-free nonlinear model predictive control based on moving horizon estimation. *Ind Eng Chem Res*. 2010;49:7882–7890.
12. Muske KR, Rawlings JB, Lee JH. Receding horizon recursive state estimation. In: Proceedings of the American Control Conference. San Francisco, CA, Institute of Electrical and Electronics Engineers (IEEE), 1993:900–904.
13. Rao CV, Rawlings JB. Constrained process monitoring: moving-horizon approach. *AIChE J*. 2002;48:97–109.
14. Qu CC, Hahn J. Computation of arrival cost for moving horizon estimation via unscented Kalman filtering. *J Process Control*. 2009;19: 358–363.
15. Ungarala S. Computing arrival cost parameters in moving horizon estimation using sampling based filters. *J Process Control*. 2009;19: 1576–1588.
16. Lopez-Negrete R, Patwardhan SC, Biegler LT. Constrained particle filter approach to approximate the arrival cost in moving horizon estimation. *J Process Control*. 2011;21:909–919.
17. Liu J. Moving horizon state estimation for nonlinear systems with bounded uncertainties. *Chem Eng Sci*. 2013;93:376–386.

18. Zhang XW, Chan SH, Ho HK, Li J, Li G, Feng Z. Nonlinear model predictive control based on the moving horizon state estimation for the solid oxide fuel cell. *Int J Hydrogen Energy*. 2008;33:2355–2366.
19. Haverbeke N, Herpe TV, Diehl M, Van den Berghe G, De Moor B. Nonlinear model predictive control with moving horizon state and disturbance estimation-application to the normalization of blood glucose in the critically ill. In: Proceedings of the 17th IFAC World Congress. Seoul, Korea, International Federation of Automatic Control (IFAC), 2008:9069–9074.
20. Voelker A, Kouramas K, Pistikopoulos EN. Simultaneous state estimation and model predictive control by multi-parametric programming. In: Proceedings of the 20th European Symposium on Computer Aided Process Engineering. Naples, Italy: Elsevier, 2010: 607–612.
21. Michalska H, Mayne DQ. Moving horizon observers and observer-based control. *IEEE Trans Autom Control*. 1995;40:995–1006.
22. Mhaskar P, El-Farra NH, Christofides PD. Predictive control of switched nonlinear systems with scheduled mode transitions. *IEEE Trans Autom Control*. 2005;50:1670–1680.
23. Mhaskar P, El-Farra NH, Christofides PD. Stabilization of nonlinear systems with state and control constraints using Lyapunov-based predictive control. *Syst Control Lett*. 2006;55:650–659.
24. Muñoz de la Peña D, Christofides PD. Lyapunov-based model predictive control of nonlinear systems subject to data losses. *IEEE Trans Autom Control*. 2008;53:2076–2089.
25. Liu J, Muñoz de la Peña D, Christofides PD, Davis JF. Lyapunov-based model predictive control of nonlinear systems subject to time-varying measurement delays. *Int J Adapt Control Signal Process*. 2009;23:788–807.
26. Christofides PD, Liu J, Muñoz de la Peña D. *Networked and Distributed Predictive Control: Methods and Nonlinear Process Network Applications*. Advances in Industrial Control Series. London, England: Springer-Verlag, 2011:230.
27. Heidarinejad M, Liu J, Christofides PD. Economic model predictive control of nonlinear process systems using lyapunov techniques. *AIChE J*. 2012;58:855–870.
28. Tabuada P. Event-triggered real-time scheduling of stabilizing control tasks. *IEEE Trans Autom Control*. 2007;52:1680–1685.
29. Anta A, Tabuada P. To sample or not to sample: self-triggered control for nonlinear systems. *IEEE Trans Autom Control*. 2010;55: 2030–2042.
30. Millan Gata P, Orihuela Espina L, Muñoz de la Peña D, Vivas C, Rubio FR. Self-triggered sampling selection based on quadratic programming. In: Proceedings of the 18th IFAC World Congress. Milan, Italy, International Federation of Automatic Control (IFAC), 2011:8896–8901.
31. Visioli A. *Practical PID Control*. London, UK: Springer, 2006.
32. Chartrand R. Numerical differentiation of noisy, nonsmooth data. *ISRN Appl Math*. 2011;2011:1–11.
33. Khalil HK. *Nonlinear Systems*, 3rd ed. Upper Saddle River, NJ: Prentice Hall, 2002.
34. Isidori A. *Nonlinear Control Systems: An Introduction*, 3rd ed. Berlin-Heidelberg: Springer-Verlag, 1995.
35. Shahmansoorian A. Inverse optimal control and construction of control Lyapunov functions. *J Math Sci*. 2009;161:297–307.
36. Mahmood M, Mhaskar P. On constructing constrained control Lyapunov functions for linear systems. *IEEE Trans Autom Control*. 2011;56:1136–1140.
37. Sun Y, El-Farra NH. Quasi-decentralized model-based networked control of process systems. *Comput Chem Eng*. 2008;32:2016–2029.
38. Mhaskar P, Liu J, Christofides PD. *Fault-Tolerant Process Control: Methods and Applications*. London, England: Springer-Verlag, 2013.
39. Ciccarella G, Dalla Mora M, Germani A. A Luenberger-like observer for nonlilear systems. *Int J Control*. 1993;57:537–556.

Manuscript received Apr. 14, 2013, and revision received Jun. 21, 2013.